16th World Conference on Earthquake Engineering, 16WCEE 2017
Santiago Chile, January 9th to 13th 2017
Paper N° 4018
Registration Code: S-A1463324900

DEVELOPING A NEW BAMBOO-SHAPE BUCKLING-RESTRAINED BRACE

Chun-Lin Wang[(1)], Li Zhou[(2)] and Ye Liu[(3)]

Key Laboratory of Concrete and Prestressed Concrete Structures of the Ministry of Education, Southeast University, Nanjing 210096, China

[(1)]chunlin@seu.edu.cn [(2)] zhouli_seu@126.com [(3)] dnliuye@126.com

Abstract

Precast concrete frames can bring tremendous benefits to a project in terms of its speed of construction, quality of finish, durability, thermal mass properties and whole life costs. But the seismic performance of precast concrete frames, especially with dry connections, remains a challenging issue. On the other hand, Buckling-Restrained Brace (BRB) is a special type of brace with global buckling inhibited by an appropriate restraining system, which implies a compression hysteretic behavior similar to the response exhibited under tension. Therefore, we focus on the employment of BRBs in the precast pre-stressed concrete frames. In this paper, experimental studies on a new bamboo-shape buckling-restrained brace (BBRB) are being conducted. BBRB specimens show stable and symmetric hysteretic behavior, whose cumulative plastic deformation exceeds the requirements specified in the AISC. The length of the slub mainly affects the end rotation of the segment. The longer slub provides smaller end rotation, making the segment more stable. The length of the segment served as energy dissipation part should be controlled in an appropriate range because too long segment can lead to the increase of local deformation of the segment and the decrease of low-cycle behavior.

Keyword: *buckling-restrained brace, bamboo-shaped, low-cycle fatigue performance*

1. Introduction

The increasing concern on structural damage control has initiated after the destructive 1994 Northridge and the 1995 Kobe earthquakes, and damage control design for building engineering and bridge engineering with the help of energy dissipation devices has been of great popularity in the last few decades. Buckling-Restrained Braces (BRBs), being a type of axial hysteretic damper, exhibits extremely stable hysteretic behavior through inelastic deformation under cyclic tension and compression loads. There are more and more behavior investigations and system applications of BRBs, which proves that the implementation of BRBs in both building [1-2] and bridge engineering [3-4] is of real use.

Numerous experimental and numerical studies at component and structure levels aim at promoting the application of various kinds of BRBs. The required stiffness of both connections and girder to prevent out-of-plane buckling was addressed based on the observation of experimental results by Kinoshita *et al*. [5]. The pseudo-dynamic tests of a full-scale 3-story 3-bay concrete filled tube (CFT)/buckling-restrained braced frame (BRBF) specimen were carried out by Tsai *et al* [6] , and the experimental responses of BRBs and BRB-to-gusset connections were focused. In particular, Usami *et al* [7] performed a series of tests that five BRB specimens were investigated to examine the validity of the currently used verification method for low-cycle fatigue of BRBs. More recently, Wang *et al* [8] studied the torsional buckling of the end portion of the partly-welded BRB and proposed a theoretical formula of the critical stress. All-steel buckling-restrained braces were tested by Chen *et al* [9] and the effect of the unbonding materials on the performance of BRBs was discussed.

A series of tests including 6 Bamboo-shaped Buckling-Restrained Brace (BBRB) specimens was performed to compare the important design parameters and address the low-cycle fatigue performance. The

details of specimens, the test set-up, the loading patterns and the test results are summarized as follows.

2. SPECIMEN SELECTION AND CLASSIFICATION

2.1 Configuration of buckling-restrained braces

Referring to Fig. 1(a), a novel BBRB consists of an inner Bamboo-shaped Core (BC) and an outer Hollow circular Tube (HT). Typically, the BC is composed of a succession of several slubs and segments depicted in Fig. 1(a), where slubs are designed to control the deformation pattern of the BC. The transition slub is set between the segment and the fixed end to spare enough space for MTS's fixtures moving back and forth and ensure the stability for BBRB core extension. From the cross-section details of the BBRB shown in Fig. 1(b), it is clear to find that the BC is surrounded by the HT and the small gap provided between the slub and the HT. At the junction of segments and slubs, some fillets shown in Fig. 1(a) are added to mitigate the stress concentration. Moreover, an opening with radius of 1.5mm in the middle slub is prepared for the stopper pin which is made of a nail with a radius of 1.4mm and length of 40mm, preventing the relative movement between the HT and the BC in the longitudinal direction during the tests. As is shown in Fig. 1(a), the red paint depicted in red color is employed on the surface of segments to apparently show any possible contact between segments and the HT.

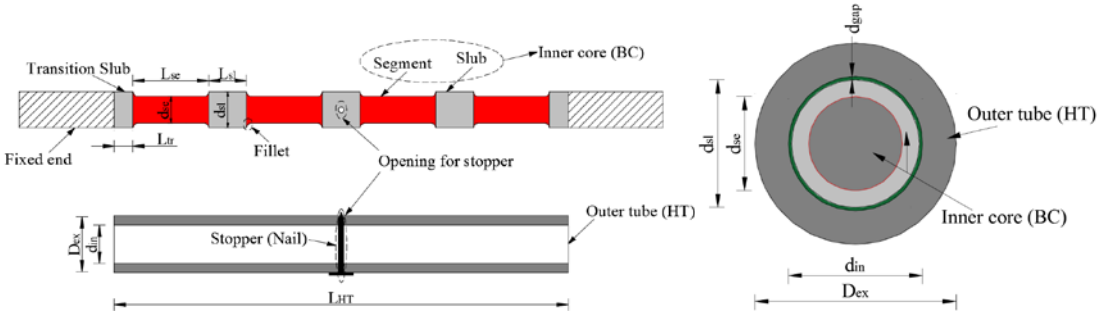

(a) assembly of BBRB (b) cross-section details

Fig. 1 Details of BBRB: (a) assembly of BBRB and (b) cross-section details.

2.2 Material characteristics

The material properties achieved from coupon tests for Q235 steel are listed in Table 1.

Table 1 Material properties of Q235 steel

Steel Batch	E (GPa)	σ_y (MPa)	σ_u (MPa)	ε_u (%)
Q235	208.4	284.3	415.6	39.4

Note: E is initial Young's modulus; σ_y is yield stress; σ_u is ultimate tensile strength; ε_u is ultimate tensile strain.

2.3 Design of BC and HT

Dimensions of bamboo-shaped core (BC) and hollow circular tube (HT) are given in Table 2. To make full use of the deformation controlling ability of the slub and the energy dissipation capacity of the segment, the slub shall be designed to remain elastic and the segment can be plastic under low-cycle load. The ratio of the sectional area of the slub to the sectional area of the segment should be controlled more than the ratio of σ_u to σ_y. In the present study, the segment is viewed as stub which is prevented from buckling. No mortar is employed between the BC and the HT.

Table 2 Measured geometric dimensions of BCs and HTs

Specimens	l	l_e	l_p	D_0	D_1	l_t	Loading Pattern
BRB40-20-1	380	20	40	19	14	260	1
BRB60-20-1	460	20	60			340	1
BRB40-20-2	380	20	40			260	2
BRB60-20-2	460	20	60			340	2
BRB40-5-1	330	5	40			210	1
BRB60-5-1	410	5	60			290	1

Note: l is the d_{sl} is the length of the segment; l_e is the length of the slub; l_p is the length of the segment; D_0 is external diameter of the HT; D_1 is the inner diameter of the HT.

2.4 Labeling

Each specimen is labelled in a fixed way. The symbols of three numbers in the labels respectively refer to the length of segment, the length of the slub and the loading pattern.

3. Low-cycle Fatigue Test Method

3.1 Testing setup

A vertical testing setup composed of a bamboo-shaped core (BC) and a hollow circular tube (HT) was previously constructed for cyclic testing and was fixed to the hydraulic servo universal testing machine MTS 810, capable of producing up to 250kN loading and maximum displacement of ±300mm. During a typical experiment, axial displacement and force of the specimens were automatically collected by a digital data acquisition system.

3.2 Loading patterns

In the present study, two different tensile and compressive reversed cyclic loading patterns illustrated were applied to these specimens. The first loading Pattern 1 consists of a stepwise incremental cyclic loading protocol. The strain amplitude of each two cycles increases from 0.5% to 4.0% with the increment 0.5% and maintains the strain amplitude 3.0% until failure. The other loading Pattern 2 is a constant strain amplitude whose strain amplitude is 3%.

4. EXPERIMENTAL RESULTS AND DISCUSSION

4.1 Low-cycle fatigue performance

The experimental force-displacement hysteresis curves are presented in Fig. 2. All testing specimens demonstrate stable and repeated hysteretic capacity, without any local or overall buckling occurrence during the loading histories even at the maximum strain amplitude. The axial forces of BRB increase with the increasing axial displacements of the BBRB, and no distinct stiffness and strength degradation occur during the test. Test results of all specimens in Table 3.

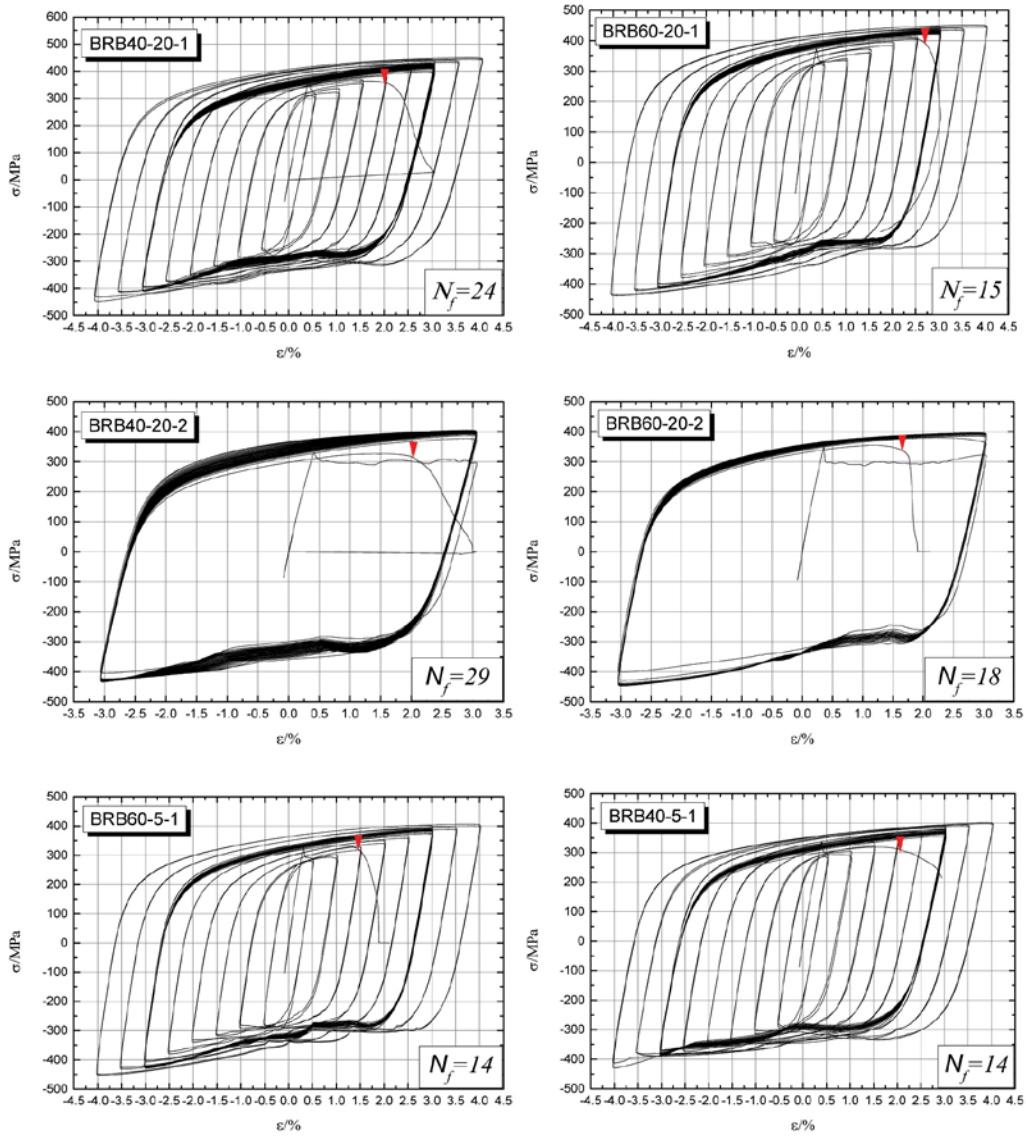

Fig. 2 Force-displacement hysteresis curves of BRB specimens

Table 3 Test results of BBRB specimens

Specimens	N_f	Loading Pattern	CPD	Failure Conditions
BRB40-20-1	24	1	3017	End
BRB60-20-1	15	1	2259	End
BRB40-20-2	29	2	2443	Middle
BRB60-20-2	18	2	1517	Middle
BRB40-5-1	14	1	2175	Middle
BRB60-5-1	14	1	2175	Middle

Note: $CPD = \sum_{i=1}^{n} [2(\Delta_{max} + \Delta_{min}) / \Delta_y - 4]$, where Δ_{max} is the maximum compressive displacement amplitude in the i_{th} hysteresis loop; Δ_{min} is the maximum tensile displacement amplitude in the i_{th} hysteresis loop; Δ_y is the yield displacement of the brace.

From the comparison of the N_f of BRB40-20-1and BRB60-20-1 or BRB40-20-2 and BRB60-20-2, it is found that the N_f decreases with the increasing length of the segment under the same strain amplitude. This demonstrates that the deformation ability of BRB is highly affected by the length of segment, and longer

segment often results in more severe local deformation making the reduction of low-cycle behavior. The N_f of BRB40-20-1 is 71.4% more than that of BRB40-5-1, which demonstrates that better deformation confining ability generated by the longer slub can reduce the deformation of the segment. Further, the better low-cycle behavior of the BBRB can be achieved. The same conclusion is also attained from the comparison between the N_f of BRB60-20-1 and the N_f of BRB60-5-1.

Among all the specimens, BRB40-20-1 has the best hysteretic behavior, proving that both smaller segment and longer slub are beneficial to the low-cycle behavior. As listed in the Table 3, the specimens with 40-mm segment have larger CPD than specimens with 60-mm segment under loading pattern 1. The same failure positions of specimens with 40-mm segment and 60-mm segment are observed in the present test. Specimens with 5-mm slub, however, exhibit relative worse hysteretic behavior. Especially, the hysteretic behavior of BRB40-5-1 is even similar to BRB60-5-1, which is different from the comparison between BRB40-20-1 and BRB60-20-1. The failure positions of specimens with 5-mm slub always initiate from the middle of the segment, while the failure positions of specimens with 20-mm slub often initiate from the end of the segment. It is clear that two different deformation modes can be explored from the experimental observation of specimens with two different length of slubs. When the rotation of the slub is small enough, the first type of deformation mode, Single-wave Deformation Mode (SDM), is formed and finally controls the deformation pattern and the hysteretic behavior of the BBRB. As is shown in Fig. 3, only single wave can generate between two adjacent restrained slubs.

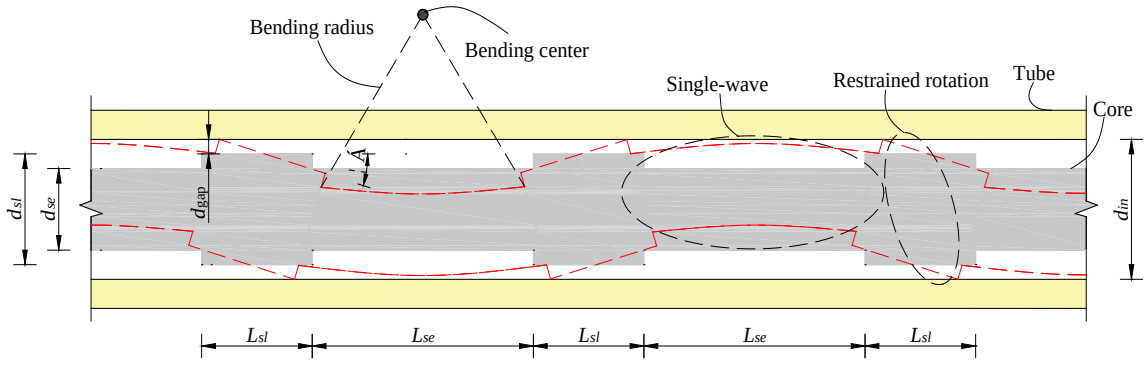

Figure 3: Single-wave Deformation Mode

Another failure mode of interest is Multi-wave Deformation Mode (MDM). As indicated in Fig. 4, due to the existence of non-restrained slubs, the core of BBRB specimen finally develops into the multi-wave form, which is different from specimens with 20-mm slub.

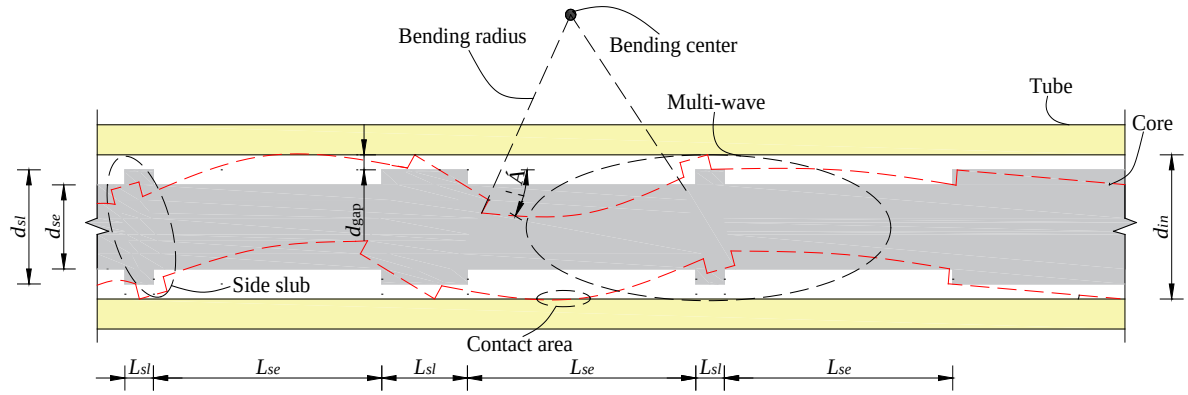

Figure 4: Multi-wave Deformation Mode (MDM)

5. Conclusions

In the present study, 6 specimens in all were tested to investigate the low-cycle behavior of BBRB, while the design parameters of these specimens were compared to provide an effective way to fabricate novel BBRB specimens. The main results are summarized as follows:

1. BBRB specimens show stable and symmetric hysteretic behavior, whose CPD exceeds the requirements specified in the AISC.
2. The length of the slub mainly affects the end rotation of the segment. The longer slub provides smaller end rotation, making the segment more stable.
3. The length of the segment served as energy dissipation part should be controlled in an appropriate range because too long segment can lead to the increase of local deformation of the segment and the decrease of low-cycle behavior.

Acknowledgements

The authors would like to acknowledge financial supports from National Natural Science Foundation of China (51678138), Natural Science Foundation of Jiangsu Province of China (BK20151407), A Project Funded by the Priority Academic Program Development of Jiangsu Higher Education Institutions.

References

[1] Iwata M, Murai M (2006): Buckling‐restrained brace using steel mortar planks; performance evaluation as a hysteretic damper [J]. Earthquake engineering & structural dynamics, **35**(14): 1807-1826.
[2] Xie Q, Zhou Z, Huang JH, Meng SP(2016) : Influence of tube length tolerance on seismic responses of multi-storey buildings with dual-tube self-centering buckling-restrained braces [J]. Engineering Structures, **116**: 26-39.
[3] Carden L P, Itani AM, Buckle IG (2006) : Seismic performance of steel girder bridges with ductile cross frames using buckling-restrained braces. Journal of Structural Engineering, **132**(3), 338-345.
[4] Usami T, Lu Z, Ge HB(2005): A seismic upgrading method for steel arch bridges using buckling-restrained braces. Earthquake Engineering & Structural Dynamics, **34**(4-5), 471–496.
[5] Kinoshita T, Koetaka Y, Inoue K, Iitani K. (2007). Criteria of buckling-restrained braces to prevent out-of-plane buckling. Journal of Structural and Construction Engineering, (621), 141-148.
[6] Tsai K, Hsiao P (2008). Pseudo-dynamic test of a full-scale CFT/BRB frame-part II: Seismic performance of buckling-restrained braces and connections. Earthquake Engineering & Structural Dynamics, 37(7), 1099-1115.
[7] Usami T, Sato T (2010). Low-cycle fatigue tests and verification method for a steel buckling-restrained brace. Journal of Structural Engineering, 56A, 486-498 (in Japanese).
[8] Wang CL, Li T, Chen Q, Wu J, Ge HB (2014). Experimental and Theoretical Studies on Plastic Torsional Buckling of Steel Buckling-restrained Braces. Advances in Structural Engineering, 17(6): 871-880.
[9] Chen Q, Wang CL, Meng SP, Zeng B. Effect of the unbonding materials on the mechanic behavior of all-steel buckling-restrained braces. Engineering Structures, 111: 478–493, 2016